

Document downloaded from:

<http://hdl.handle.net/10251/51946>

This paper must be cited as:

Martinez Franco, R.; Moliner Marin, M.; Franch Martí, C.; Kustov, A.; Corma Canós, A. (2012). Rational direct synthesis methodology of very active and hydrothermally stable Cu-SAPO-34 molecular sieves for the SCR of NO_x. *Applied Catalysis B: Environmental*. 127:273-280.



The final publication is available at

<http://dx.doi.org/10.1016/j.apcatb.2012.08.034>

Copyright Elsevier

**Rational direct synthesis methodology of very active and hydrothermally stable Cu-
SAPO-34 molecular sieves for the SCR of NOx.**

Raquel Martínez-Franco¹, Manuel Moliner^{1*}, Cristina Franch¹, Arkady Kustov², Avelino
Corma^{1*}

¹ Instituto de Tecnología Química (UPV-CSIC), Universidad Politécnica de Valencia,
Consejo Superior de Investigaciones Científicas, Valencia, 46022, Spain

² Haldor Topsøe A/S, Nymøllevej 55, DK-2800 Lyngby, Denmark

*Corresponding authors: E-mail addresses: acorma@itq.upv.es; mmoliner@itq.upv.es

Abstract

A one-pot direct synthesis of Cu-SAPO-34 has been achieved that allows more than 90% yield in the material synthesis. By this method it is easy to control the Cu-loading in the Cu-SAPO-34. It is presented that a maximum in hydrothermal stability with very high activity for NO_x SCR with NH₃ is obtained for an optimum Cu loading.

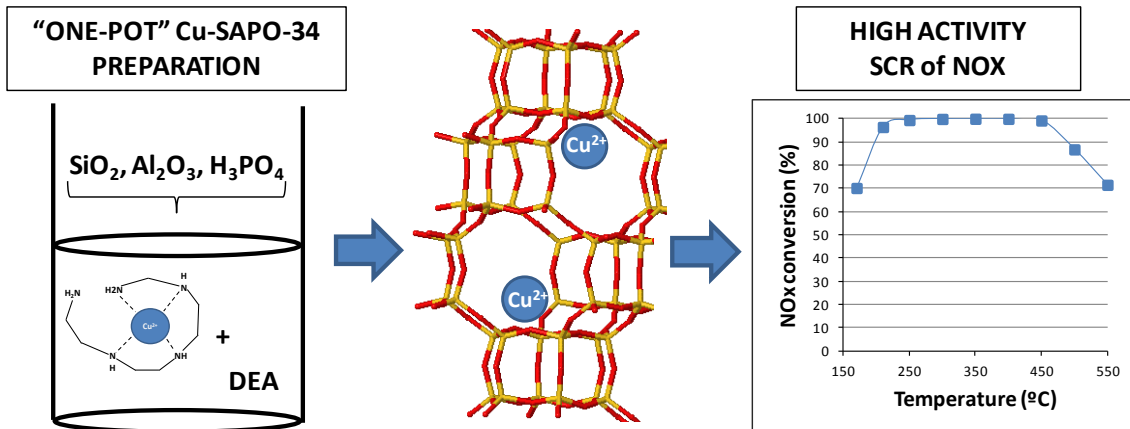
Keywords

One-pot synthesis, silicoaluminophosphate, SAPO-34, selective catalytic reduction (SCR), nitrogen oxides (NO_x)

Highlights

- Rational direct synthesis of Cu-SAPO-34 by using the co-directing templates.
- Easy control of Cu-loading in Cu-SAPO-34 materials, and very high solid yields.
- High activity and stability for SCR of NO_x.

Graphical abstract



1.- Introduction

Nitrogen oxides (NO_x), involving nitric oxide (NO), nitrogen dioxide (NO₂) and nitrous oxide (N₂O) are major air pollutants [1]. NO_x is generated primarily by the combustion of fossil fuels, both in transportation and industrial processes. However, transports, and especially those working with diesel engines, are the main sources of NO_x emissions [2]. Selective catalytic reduction (SCR) of NO_x by ammonia has become the most used emission control [3], and catalysts based on vanadia are in commercial use since 2005 for diesel vehicles [4]. However, vanadia catalysts suffer some serious drawbacks, as oxidation of SO₂ to SO₃ (which would react with H₂O resulting in H₂SO₄), and low activity and selectivity at high temperatures due to the sintering of vanadia species [5].

The discovery of copper-exchanged zeolites as active and stable catalysts for the SCR of NO_x by Iwamoto et al. introduced an attractive alternative to vanadia-based materials [6]. Several metal-exchanged molecular sieves, primary medium and large pore zeolites, have been reported in the last two decades for the SCR of NO_x [7]. Unfortunately, those materials present low hydrothermal stability when reacting under harsh conditions (presence of steam at high temperatures). Recently, BASF researchers have described that copper-containing small-pore chabazite zeolite shows much better hydrothermal stability than large pore zeolites (Cu-Beta or Cu-Y) [8]. This description has revived the industrial interest in metal-containing molecular sieves for NO_x abatement [9]. In this sense, Lobo et al. [10] have reported that the higher hydrothermal stability and better catalytic behavior of Cu-CHA for SCR of NO_x is due to the localization of copper atoms coordinated to the double six-membered rings units (D6-MR) present in the large cavities of chabazite structure.

Conventionally, those metal-containing molecular sieves are obtained by post-synthesis ion-exchange procedures. Indeed, several steps, such as hydrothermal synthesis of the molecular sieves, calcination, metal ion exchange, and calcination are required to get the final metal-containing molecular sieves.

Recently, Xiao et al [11] have nicely reported the direct preparation of Cu-SSZ-13 zeolite (SSZ-13 is the silicoaluminate form of the CHA structure) by using a low-cost

copper-amine complex (Cu^{2+} with tetraethylenepentamine, Cu-TEPA) as an efficient template. This methodology allowed the direct introduction of extra-framework copper species in the CHA cages, revealing promising results in SCR of NO_x reaction. Despite the remarkable impact that this discovery could have on the NO_x field, the materials reported in this manuscript suffer from important drawbacks. SSZ-13 syntheses with several Si/Al ratios (5, 7.5, 12.5, and 17.5) were attempted, but the final Si/Al ratios into the solids were much lower (4.1, 4.3, 5.3, and 7.5, respectively). These values clearly indicate that large part of the initially introduced silicon species remained in solution when the Si/Al ratio was increased, notoriously affecting to the SSZ-13 yield. Moreover, the desired industrial catalysts for the SCR of NO_x must show high hydrothermal stability due to the reaction conditions, i.e. high temperature and presence of steam. It is well known that zeolites with low Si/Al ratio (less than 10) suffer severe dealumination processes in presence of steam at high temperature [12]. In fact, the SCR of NO_x experiment described by Xiao was performed on the sample with Si/Al ratio of 4.1 under mild conditions (low space velocity), and the stability of the synthesized samples under hydrothermal treatments was not studied. Furthermore, the different Cu-SSZ-13 examples reported by Xiao et al. show similar Cu loadings ($\text{Cu}/\text{Si} = 0.09\text{-}0.10$), indicating that the amount of Cu on SSZ-13 samples cannot be easily varied in a controlled manner.

In addition to SSZ-13, the chabazite molecular sieve can be synthesized as silicoaluminophosphate form, SAPO-34 [13]. Cu-exchanged SAPO-34 has also been shown as a very stable and active material for SCR of NO_x [14]. In the last years, some groups have attempted the direct preparation of Cu-SAPO-34 in order to achieve an inexpensive and more efficient synthetic route for this metal-substituted material [15]. In those cases morfoline and copper oxide were used as organic structure directing agent (OSDA) and copper source, respectively. Those crystalline Cu-SAPO-34 materials show very low Cu contents [$\text{Cu}/(\text{Al}+\text{P}) = 0.02$], and samples with higher Cu loadings direct into amorphous materials, low solid yields (lower than 70% of initial sources), and mixture of metal in framework positions and extra-framework cationic positions.[15c] During the preparation of the present manuscript, a very interesting paper studying the effect of the synthesis approach (cation exchange, chemical vapor

deposition and direct synthesis) on the nature of the Cu active site, and therefore, on the SCR of NO_x activity, has been published.[16] In that work, the authors showed the direct synthesis preparation of Cu-SAPO-34 material by using a combination of templates, such as the Cu²⁺-triethylenetetramine complex and tetraethylammonium cations, obtaining interesting catalytic results for the SCR of NO_x. Those experiments were performed in absence of steam, and moreover, the catalyst stability tests against severe ageing treatments were not carried out.

Herein, we will show a very detailed and rationalized “one-pot” Cu-SAPO-34 preparation, from the use of a Cu-complex (Cu²⁺ with tetraethylenepentamine, Cu-TEPA) as the unique template, to the cooperative and fundamental role of a small organic molecule (as diethylamine, DEA) acting as co-template. Following this rationalized direct synthesis methodology, the Cu-loading in extra-framework positions into the material can be easily controlled, and the final solid yields obtained are very high (larger than 90% of expected solids from initial precursors). Those Cu-SAPO-34 samples are extremely active and hydrothermally stable when tested in the SCR of NO_x reaction under very severe reaction conditions (very high space velocity, and presence of steam at very high temperatures). The combination of the direct synthesis of Cu-SAPO-34 together with hydrothermal stability and excellent catalytic results obtained for the SCR of NO_x introduces new opportunities for the industrial use of this type of material.

2.- Experimental

2.1.- Synthesis

2.1.1.- Direct syntheses of Cu-SAPO-34 materials

In a general procedure for the Cu-SAPO-34 preparation, the Cu-complex was firstly prepared by mixing a 20%wt of an aqueous solution of copper (II) sulfate (98%wt, Alfa) with the tetraethylenepentamine (TEPA, 99%wt, Aldrich). This mixture was stirred for 2 hours until complete dissolution. Secondly, distilled water and phosphoric acid (85% wt, Aldrich) were added and stirred during 5 minutes. Third, alumina (75%wt, Condea)

and silica (Ludox AS40 40%wt, Aldrich) sources were introduced in the gel mixture. Finally, diethylamine (DEA, 99%wt, Aldrich) and SAPO-34 seeds (5%wt of expected final yield), if required, were added in the gel, and the mixture was stirred during 30 minutes. The resulting gel was transferred to an autoclave with a Teflon liner, and heated at 150°C under static conditions during the required time (see experimental conditions for each sample in Table 1, Table 3, or Table 4). Crystalline products were filtered and washed with abundant water, and dried at 100°C overnight. The samples were calcined at 550°C in air to properly remove the occluded organic species.

2.1.2.- SAPO-34 synthesis for post-synthesis Cu-exchange

SAPO-34 was synthesized following the procedure describe in the literature [17]. The molar gel composition was: 2 DEA: 0.6 SiO₂: 1 Al₂O₃: 0.8 P₂O₅: 50 H₂O, keeping the mixture autoclaved at 200°C during 72 hours. The resulting product was filtered and washed with distilled water, and dried at 100°C overnight. The sample was calcined at 550°C in air to remove the occluded organic species.

In order to perform the Cu ion exchange on this SAPO-34 material, the calcined sample was first washed with NaNO₃ (0.04M), and afterwards, the sample was exchanged at room temperature with a Cu(CH₃CO₂)₂ solution (solid/liquid ratio of 10g/L). Finally, the sample was filtered and washed with distilled water, and calcined at 550°C for 4 h.

2.2.- Characterization

X-ray diffraction (XRD) measurements were performed on a multisample Philips X'Pert diffractometer equipped with a graphite monochromator, operating at 40 kV and 45 mA, and using Cu K_α radiation ($\lambda = 0,1542$ nm).

The chemical analyses were carried out in a Varian 715-ES ICP-Optical Emission spectrometer, after solid dissolution in HNO₃/HCl/HF aqueous solution. The organic content of as-made materials was determined by elemental analysis performed on a SCHN FISIONS element analyzer. Thermogravimetric analysis was evaluated using a Mettler Toledo thermo-balance.

Textural properties were determined by N₂ adsorption-desorption isotherms measured on a Micromeritics ASAP 2020 at 77 K.

The morphology of the samples was studied by scanning electron microscopy (SEM) using a JEOL JSM-6300 microscope.

The NMR spectra were recorded at room temperature on a Bruker AV 400 spectrometer MAS. ^{29}Si NMR spectra were recorded with a spinning rate of 5 kHz at 79.459 MHz with a 55° pulse length of 3.5 μs and repetition time of 180 s. ^{27}Al MAS NMR spectra were recorded at 104.2 MHz with a spinning rate of 10 kHz and a 9° pulse length of 0.5 μs with a 1 s repetition time. Solid-state ^{31}P NMR spectra were recorded at 161.9 MHz with a spinning rate of 10 kHz, a $\pi/2$ pulse of 5 μs with 20 s repetition time.

^{29}Si , ^{27}Al and ^{31}P chemical shifts were referred to tetramethylsilane, $\text{Al}^{3+}(\text{H}_2\text{O})_6$, and 85% H_3PO_4 , respectively.

2.3.- Catalytic experiments.

The activity of the samples for the selective catalytic reduction of NO_x using NH_3 as reductor was tested in a fixed bed, quartz tubular reactor of 2.2 cm of diameter and 53 cm of length. The total gas flow was fixed at 300 ml/min, containing 500 ppm of NO , 530 ppm of NH_3 , 7% of O_2 , and 5% of H_2O . The catalyst (40 mg) was introduced in the reactor, heated up to 550 $^\circ\text{C}$ and maintained at this temperature for one hour under nitrogen flow. After that the desired reaction temperature was set (170-550 $^\circ\text{C}$) and the reaction feed admitted. The NO_x present in the outlet gases from the reactor were analyzed continuously by means of a chemiluminescence detector (Thermo 62C).

2.4.- Steaming procedures

The hydrothermal stability of metal-containing molecular sieves was studied by steaming with water (2.2 mL/min) at 600 $^\circ\text{C}$ or 750 $^\circ\text{C}$ during 13 hours in an oven.

3.- Results

3.1.- Direct synthesis of Cu-SAPO-34 using Cu-TEPA as the unique organic template.

We have first studied the use of the Cu-complex formed by Cu^{2+} with tetraethylenepentamine (TEPA) in the typical synthesis conditions of SAPO-34 as the unique organic template. Two different molar ratios of Cu-complex, three of water, and two P/Al ratios [and consequently two Si/(P+Al)] were screened in order to synthesize Cu-SAPO-34 by a “one-pot” methodology. The experimental design performed is summarized in Table 1.

As it can be seen in Figure 1, Cu-SAPO-34 materials were only achieved when a large amount of complex was introduced in the synthesis media [$\text{Cu-TEPA}/(\text{Al+P})=0,5$]. If the Cu-complex content was reduced [$\text{Cu-TEPA}/(\text{Al+P})=0,2$], amorphous materials were obtained. Figure 2 shows the XRD patterns of the SAPO34-1 (as referred in Figure 1) in as-prepared form and after calcination in air at 550°C. The XRD patterns confirm the CHA structure of those samples, and also reveal their stability after regular calcinations in air at 550°C. The other synthesized Cu-SAPO-34 samples in the present study (see Figure 1), show similar XRD patterns.

Chemical analyses were performed on synthesized Cu-SAPO-34 materials in order to study their real Cu-content. As seen in Table 2, SAPO34-1 and SAPO34-4 samples show higher Cu-contents [$\text{Cu}/(\text{Al+P})=0.21$] than the other SAPO34 samples [$\text{Cu}/(\text{Al+P})=0.13-0.14$]. It seems that under these synthesis conditions, the gel dilution plays an important role in the Cu-loading, achieving larger Cu-loadings for lower water content [$\text{H}_2\text{O}/(\text{Al+P})=10$]. Elemental analyses indicate that the occluded organic molecules (TEPA) remain intact after the crystallization processes (see experimental C/N ratios in Table 2).

SAPO34-1 and SAPO34-6 samples, both prepared under very different synthetic conditions and also containing different copper loadings (see Table 2), were selected to study their catalytic behavior on the SCR of NO_x reaction. Those samples show medium-activity (see Figure 3) when tested with of 5% of water in the feed and very high gas hourly space velocity, 450,000 $\text{ml}/\text{h.g}_{\text{cat}}$. However, SAPO34-6, which contains lower Cu-loading in the solid, presents better activities at high temperatures. More interestingly, SAPO34-6 shows similar activity than Cu-exchanged SAPO-34 (see experimental section for details). Those results clearly indicate the importance of controlling the Cu amount in extra-framework positions into the final solids for the catalytic activity on the SCR of NO_x .

3.2.- Direct synthesis of Cu-SAPO-34 using different amounts of Cu-TEPA with an excess of TEPA molecules.

As reported above, the large amount of copper-complex required in the synthesis media [$\text{Cu-TEPA}/(\text{Al+P}) = 0.5$] to achieve Cu-SAPO-34 materials promotes a very large loading of copper in the final solid [$\text{Cu}/(\text{Al+P})$ between 0.13-0.21, see Table 2]. If Cu-TEPA complex quantity is reduced from the synthesis gel, only amorphous materials were achieved (see Figure 1). Therefore, a new strategy must be defined in order to synthesize SAPO-34 materials by direct methodologies but with controlled Cu-loadings. In this sense, we decided to prepare a new set of experiments where defined ratios of Cu-complex were fixed [$\text{Cu-TEPA}/(\text{P+Al}) = 0,1, 0,2, 0,3, 0,4$] in combination with an excess of TEPA molecules (see experimental design in Table 3), which would act as co-organic space fillers, and consequently, would permit the diminution of Cu atoms in the final crystalline materials.

Unfortunately, only mixtures of SAPO-34 and amorphous materials were obtained in all experiments when the combination of Cu-TEPA complex and TEPA molecules was used for the direct preparation of Cu-SAPO-34 materials (see Figure 4). Figure 5 shows the low crystalline nature of the achieved samples.

3.3.- Direct synthesis of Cu-SAPO-34 using different amounts of Cu-TEPA with a cooperative OSDA (diethylamine, DEA).

In order to improve the crystallization of SAPO-34 with reduced and controlled Cu-complex amounts, we decided to study the introduction of a different cooperative OSDA, such as diethylamine (DEA), which is an organic molecule widely used in the preparation of regular SAPO-34 [17]. In this sense, controlled quantities of Cu-complex [$\text{Cu-TEPA}/(\text{Al+P}) = 0.05, 0.1, 0.15$ and 0.2] were studied by adding into the mixture an excess of the cooperative organic molecule DEA, keeping constant the total amount of organic molecules [$\text{Cu-TEPA}/(\text{Al+P}) + \text{DEA}/(\text{Al+P}) = 0.5$]. The experimental design is summarized in Table 4.

As seen in Figure 6, SAPO-34 materials were obtained with different amounts of Cu-complex in the synthesis media, when the $\text{Si}/(\text{Al+P})$ ratio was fixed in 0.2, after 7 days at 150°C. Interestingly, the preparation of fully-crystalline SAPO-34 can be remarkably

improved when small amounts of SAPO-34 seeds (5%wt of expected final yield) were introduced in the mixture (see Figure 6). The XRD patterns of the as-prepared SAPO34-7, -8, and -9, synthesized with different Cu amounts in the synthesis mixture, are listed in Figure 7.

The characterization of those directly-synthesized Cu-SAPO-34 materials by UV-Vis spectroscopy confirms the stability of the Cu-complex after the crystallization. UV-Vis spectra of the Cu-TEPA complex in solution and the as-prepared Cu-SAPO-34 materials exhibit a strong band at 270 nm, revealing that Cu-TEPA complex is retained intact after crystallization inside the SAPO-34 materials (see Figure 8). Those occluded Cu-complex molecules lead the presence of cationic copper extra-framework species after organic removal by calcination.

Chemical and elemental analyses were performed on those three Cu-SAPO-34 materials synthesized by the cooperative OSDA direct methodology (see Table 5). Those analyses demonstrate that different and controlled loading of copper into the final solids is obtained by following the present methodology [see Cu/(P+Al) in Table 5]. Moreover, a good correlation between the amount of DEA and TEPA into the final solids is found depending on the initial theoretical ratio of Cu-TEPA (the larger the theoretical Cu-TEPA ratio, the higher the content of TEPA into the final solid), clearly evidencing a controlled insertion of the Cu-complex during the nucleation-crystallization processes.

More importantly, the final solid yields of the Cu-SAPO-34 materials obtained after their calcination are higher than 90%. Those values are much higher than previously reported yields on the direct synthesis of Cu-SAPO-34 provided by researchers at BASF (~70%) [15c].

SEM images of the three directly-synthesized Cu-SAPO-34 materials reveal cubic crystals with similar averaged sizes (6-10 μm).

The catalytic activity of those Cu-SAPO-34 materials was studied under severe catalytic conditions (presence of 5% of water in the feed and very high gas hourly space velocity, 450,000 ml/h.g_{cat}). As reported in Figure 10, those materials proceed very well for the SCR of NO_x. Particularly, SAPO34-8 shows an exceptional catalytic profile, indicating that the intermediate extra-framework Cu-loading [Cu/(Al+P) = 0.07] seems

to be the optimum metal charge for those materials. Those catalytic results clearly indicate that SAPO-34 materials, especially SAPO34-8, are very active for SCR of NO_x reaction. At this time, further analysis on the product distribution must be performed in order to study the selectivity of those materials towards the desired N₂ formation.

Additional characterization has been performed on the optimum SAPO34-8 in order to study its microporosity, and the coordination of the atoms present in the support. The N₂ adsorption isotherm at 77 K shown in Figure 11 reveals the microporous nature of SAPO34-8, with a micropore volume of 0.14 cm³/g. The coordination of the atoms present in the support was studied by solid-state NMR. ³¹P MAS NMR indicates a single signal at -28 ppm indicative of one distinguishable type of tetrahedral phosphorous (see Figure 12A). ²⁷Al MAS NMR spectrum exhibits a strong peak at 35 ppm, which corresponds to Al in tetrahedral environments in the framework,[18] while the signal at 10 ppm has been assigned to five-coordinated aluminium in the framework of SAPO-34 with water molecules (see Figure 12B).[19] Finally, ²⁹Si MAS NMR spectrum indicates that part of silicon atoms are selectively replacing phosphorous atoms in the framework (see signal at -91 ppm in Figure 12C), while the signal at -111 ppm reveals that Si-rich domains are also present in the final solid.

3.4.- Hydrothermal stability of Cu-SAPO-34 materials synthesized using different amounts of Cu-TEPA with a cooperative OSDA (diethylamine, DEA).

The hydrothermal stability of those three Cu-SAPO-34 materials synthesized using different amount of Cu-TEPA with a cooperative OSDA were further studied by performing steaming treatments at high temperatures (600 and 750°C) during 13 hours. As shown in Figure 13, all three samples show excellent hydrothermal stability when treated at 600°C in presence of steam for long time periods. The catalytic activity for SCR of NO_x was tested for those hydrothermally-treated samples, and as seen in Figure 14, both SAPO34-8 and -9 proceed with conversions higher than 90% in most of the tested temperatures, while SAPO34-7 shows conversion values close to 70%. Despite the similar activity profile between SAPO34-8 and -9, better conversions are achieved at higher temperatures when working with the former, illustrating the

enhanced catalytic behaviour of the intermediate Cu-loading SAPO-34, even after the steaming treatment.

However, when Cu-SAPO-34 materials were treated under more extreme conditions at 750°C in presence of steam for 13 hours, SAPO34-7 sample shows an excellent hydrothermal stability when compared to the other samples (see Figure 13). Indeed, it seems that there is a clear correlation between the Cu content and the hydrothermal stability of the Cu-SAPO-34 at 750°C. In this case, hydrothermally-treated SAPO34-7 material was tested on the SCR of NO_x catalyst, obtaining NO_x conversions close to 70% in a very broad temperature profile (see Figure 14). Those results are very similar to the achieved values on SAPO34-7 when was treated at 600°C, indicating that Cu environments have not significantly changed after the hydrothermal treatment at 600 or 750°C.

4.- Conclusions

The rational use of the Cu-TEPA complex combined with an additional organic molecule (as DEA) allow the inexpensive direct synthesis of Cu-SAPO-34 material with controlled Cu-loading into the final solids, and very high yields of solids after calcination (> 90 % of the expected solid). The range of Cu-loading into the final solids is much higher than with other previously reported Cu-SAPO-34 materials synthesized by direct methodologies and, importantly, those Cu atoms are primary in extra-framework cationic form (Cu-complex molecule remains unaltered inside of the as-prepared Cu-SAPO-34, as confirmed by UV-Vis spectroscopy). Moreover, those materials perform very well in the SCR of NO_x reaction, making those materials and their synthesis methodology very promising for their industrial application.

Acknowledgements

This work has been supported by Haldor-Topsoe, Consolider Ingenio 2010-Multicat, and UPV through PAID-06-11 (n.1952). MM acknowledges to “Subprograma Ramon y Cajal” for the contract RYC-2011-08972.

Figure 1: Phases obtained for the direct hydrothermal synthesis of silicoaluminophosphates by using Cu-TEPA as the unique organic template

			P/Al = 0,9 Si/(Al+P) = 0,1	P/Al = 0,8 Si/(Al+P) = 0,2
H ₂ O/(Al+P)	10	Cu-TEPA/(Al+P) — 0,2		
		— 0,5	SAPO34-1	SAPO34-4
	30	Cu-TEPA/(Al+P) — 0,2		
		— 0,5	SAPO34-2	SAPO34-5
	50	Cu-TEPA/(Al+P) — 0,2		
		— 0,5	SAPO34-3	SAPO34-6

 Amorphous
 SAPO-34

Figure 2: XRD patterns of Cu-SAPO34-1 in as-prepared and calcined form

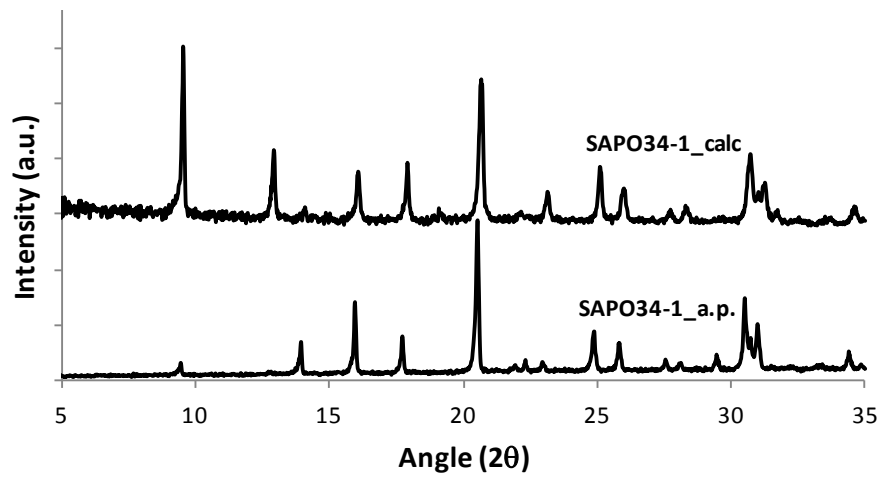


Figure 3: Catalytic activity for the SCR of NO_x reaction of Cu-SAPO-34 materials synthesized using Cu-TEPA as the unique organic molecule and Cu exchanged SAPO-34.

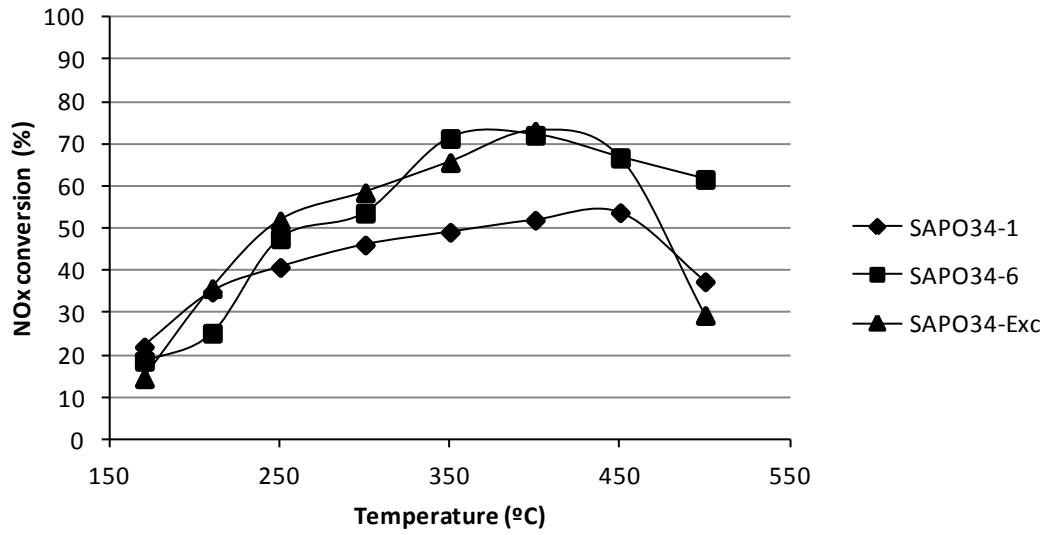


Figure 4: Phases obtained for the direct hydrothermal synthesis of Cu-SAPO-34 using different amounts of Cu-complex (Cu-TEPA) with the addition of an excess of TEPA

				P/Al = 0,9 Si/(Al+P) = 0,1	P/Al = 0,8 Si/(Al+P) = 0,2
H ₂ O/(Al+P) = 30	TEPA/(Al+P) = 0,5	Cu ²⁺ /(Al+P)	0		Non-tested
			0,1		
			0,2		
			0,3		
			0,4		


 Amorphous
 Amorphous+SAPO-34

Figure 5: XRD pattern of the most crystalline material obtained using Cu-TEPA in combination with an excess of TEPA molecules

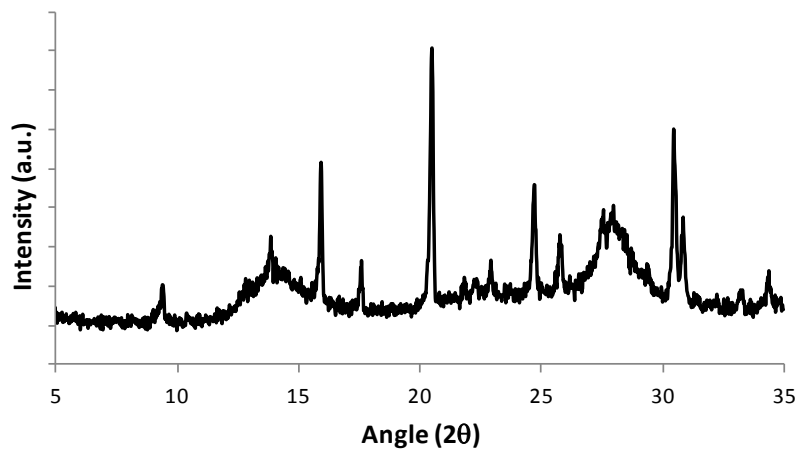


Figure 6: Phases obtained for the direct hydrothermal synthesis of Cu-SAPO-34 using different amounts of Cu-complex (Cu-TEPA) in combination with a cooperative OSDA (diethylamine, DEA)

		P/Al = 0,9 Si/(Al+P) = 0,1				P/Al = 0,8 Si/(Al+P) = 0,2					
Cu-TEPA/(Al+P)		0,05	0,1	0,15	0,2	0,05	0,1	0,15	0,2		
DEA		0,45	0,4	0,35	0,3	0,45	0,4	0,35	0,3		
H ₂ O/(Al+P) = 10		Non-tested				SAPO34-7 SAPO34-8		SAPO34-9		1 day	
										7 days	
										7 days (5%wt seeds)	


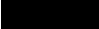

	Amorphous
	SAPO-34
	SAPO-34+Amorphous

Figure 7: XRD patterns of the synthesized Cu-SAPO-34 materials using different amounts of Cu-complex (Cu-TEPA) in combination with a cooperative OSDA (diethylamine, DEA)

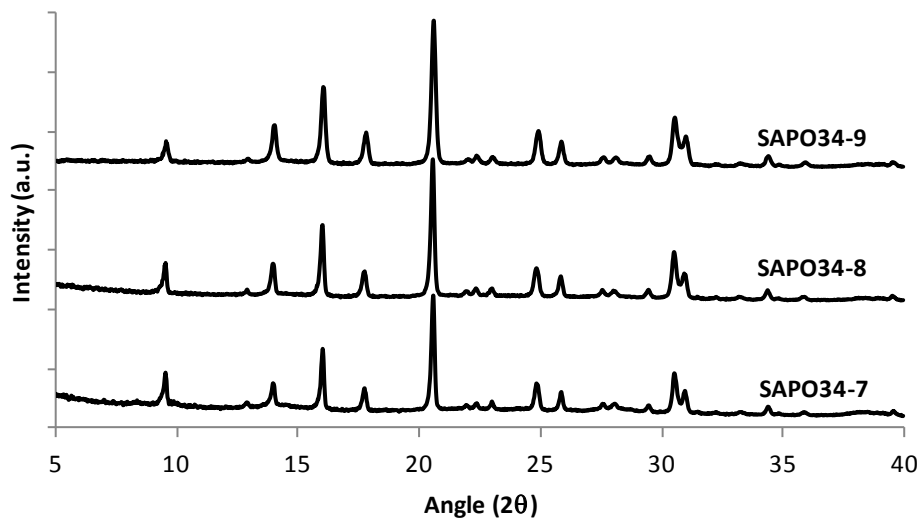


Figure 8: UV-Vis spectra of Cu-TEPA complex in solution, and as-prepared Cu-SAPO-34 materials.

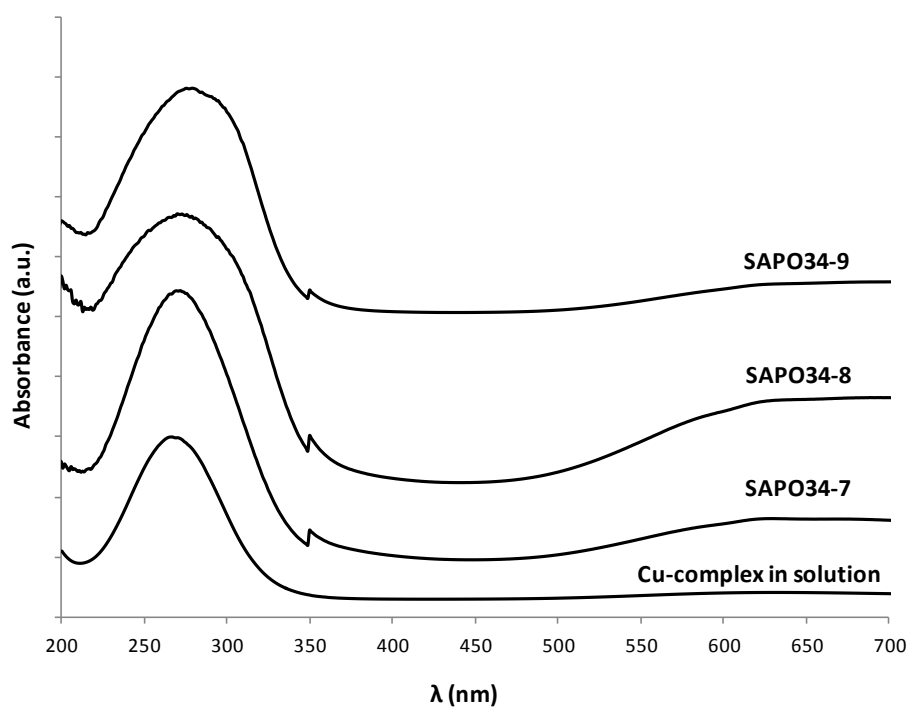


Figure 9: SEM image of (a) SAPO34-7, (b) SAPO34-8 and (c) SAPO34-9.

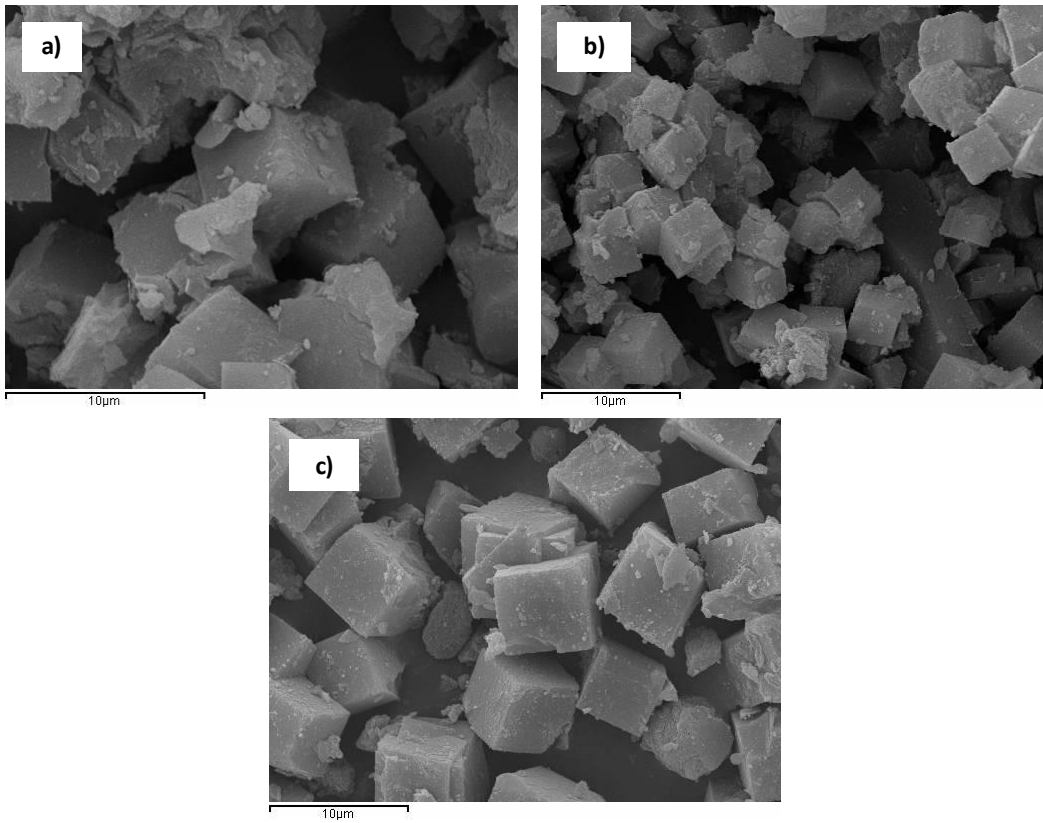


Figure 10: Catalytic activity for the SCR of NO_x reaction of Cu-SAPO-34 materials synthesized using different amounts of Cu-complex (Cu-TEPA) in combination with a cooperative OSDA (diethylamine, DEA)

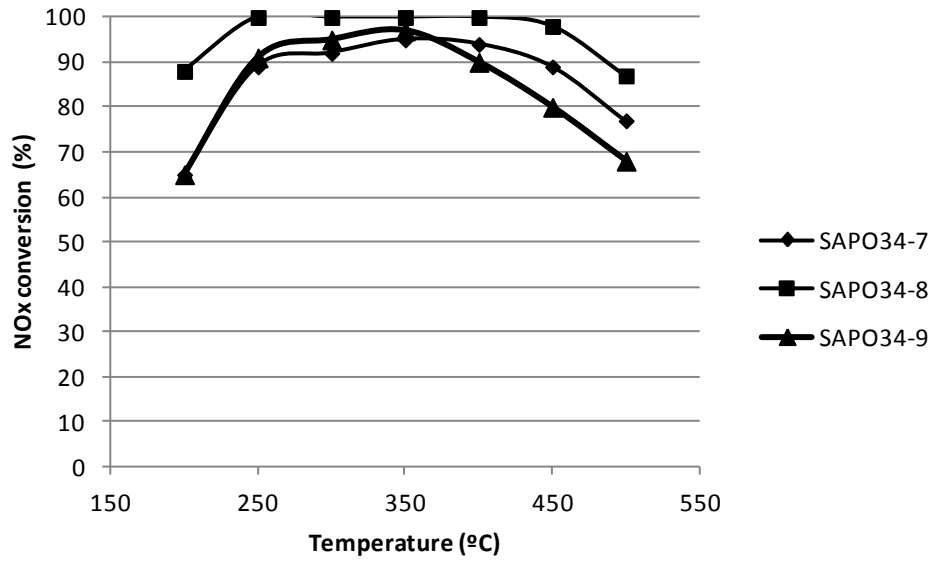


Figure 11: N₂ adsorption isotherm obtained for SAPO34-8 material

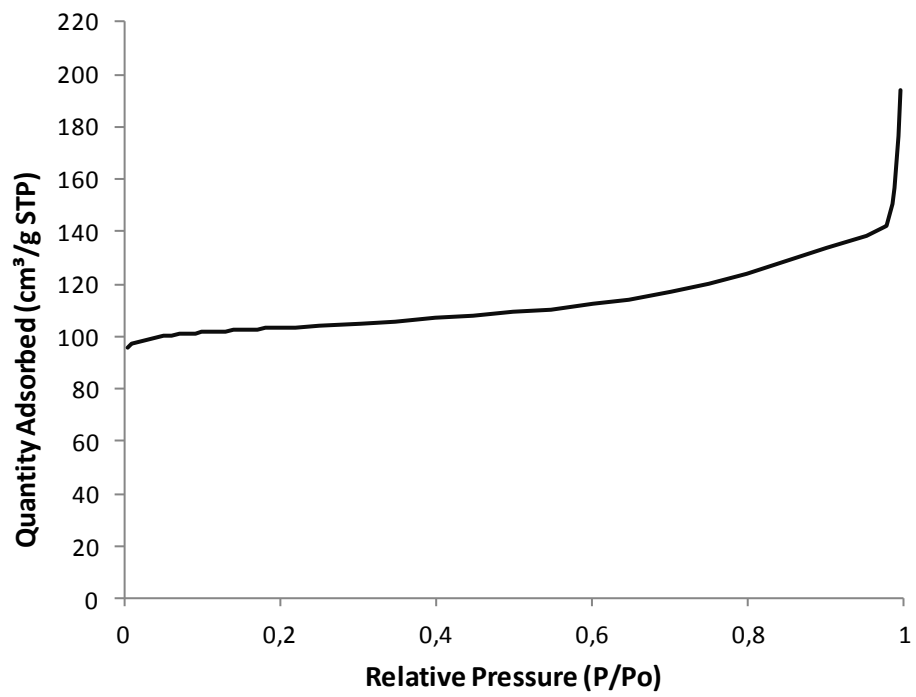


Figure 12: Solid-state NMR spectra of SAPO34-8: (a) ^{31}P MAS NMR, (b) ^{27}Al MAS NMR, and (c) ^{29}Si MAS NMR,

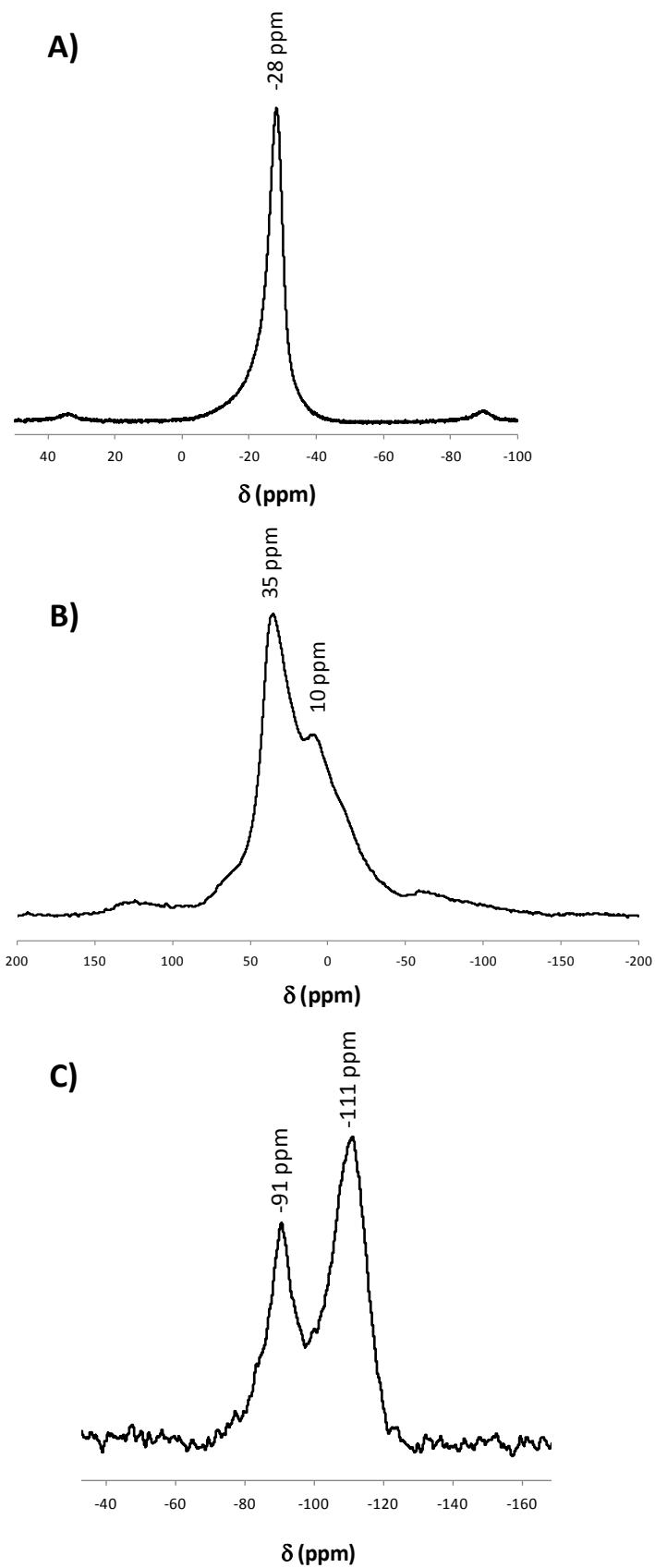


Figure 13: XRD patterns of Cu-SAPO-34 materials after severe steam treatments

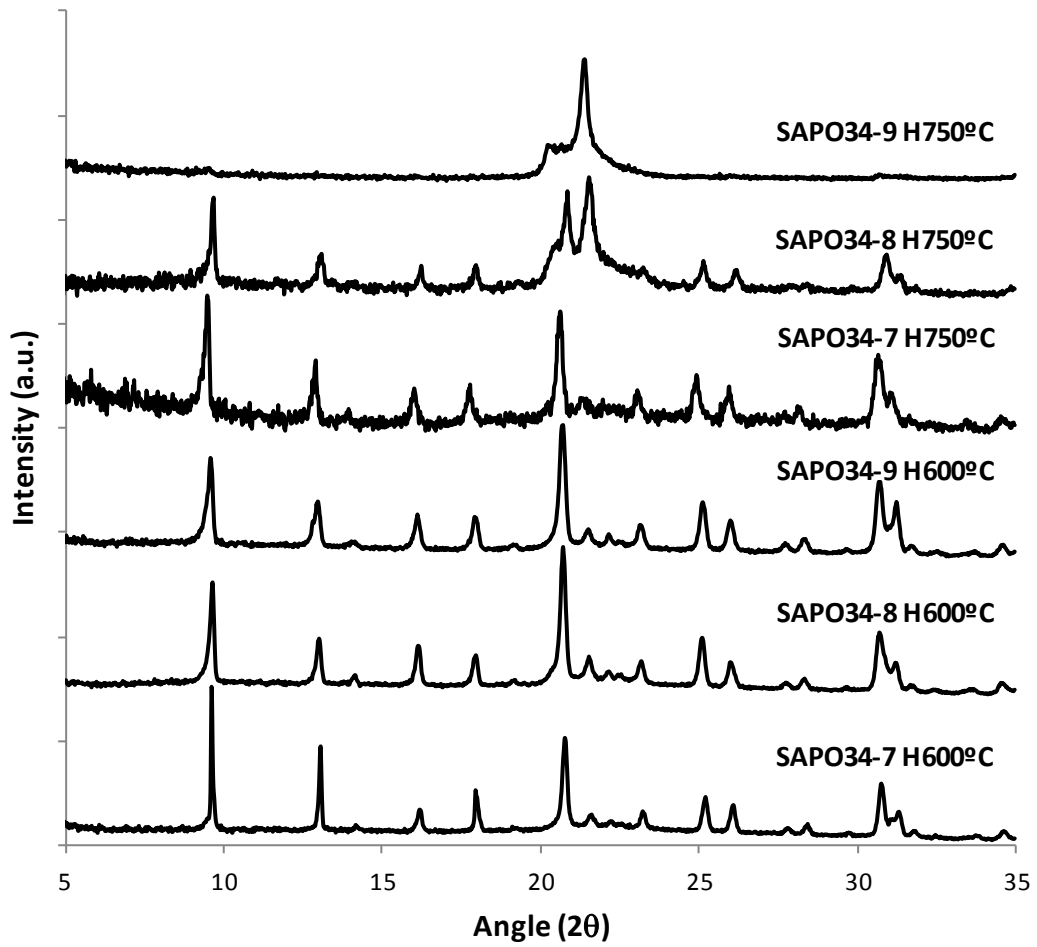


Figure 14: Catalytic activity for the SCR of NO_x reaction of Cu-SAPO-34 materials synthesized using different amounts of Cu-complex (Cu-TEPA) in combination with a cooperative OSDA (diethylamine, DEA) after steam treatments

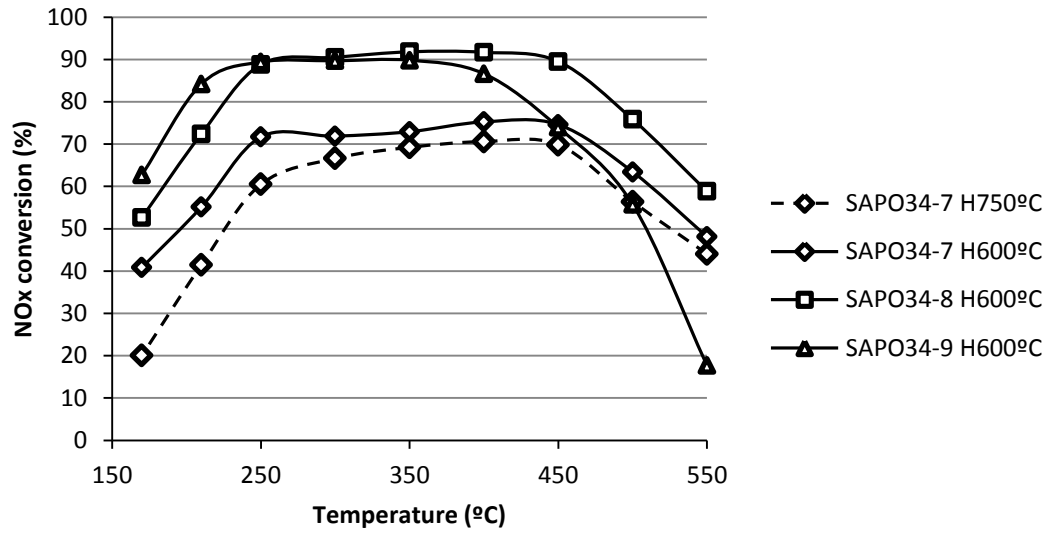


Table 1: Experimental design for the direct hydrothermal synthesis of silicoaluminophosphates by using different amounts of Cu-complex as OSDA (T = 150°C static conditions, t = 7 days)

Variable	Values
<i>Cu-TEPA/(Al+P)</i>	0.2, 0.5
<i>H₂O/(Al+P)</i>	10, 30, 50
<i>P/Al</i>	0.8, 0.9
<i>[Si/(Al+P)]</i>	[0.2, 0.1, respectively]

Table 2: Chemical and elemental analyses of Cu-SAPO-34 samples achieved by using Cu-TEPA as OSDA

Sample	Si/(Al+P)	Cu/(Al+P)	C/N)real	C/N)teor
SAPO34-1	0.27	0.21	22	1.6
SAPO34-2	0.18	0.14	1.6	1.6
SAPO34-3	0.17	0.14	1.6	1.6
SAPO34-4	0.23	0.21	1.6	1.6
SAPO34-5	0.22	0.13	1.6	1.6
SAPO34-6	0.23	0.13	1.6	1.6
SAPO34-Exc	0.15	0.07	---	---

Table 3: Experimental design for the direct hydrothermal synthesis of silicoaluminophosphates by using controlled amounts of Cu-complex and an excess of TEPA (T = 150°C static conditions, t = 7 days)

Variable	Values
<i>Cu-TEPA/(Al+P)</i>	0.1, 0.2, 0.3, 0.4
<i>[TEPA/(Al+P)]</i>	[0.4, 0.3, 0.2, 0.1, respectively]
<i>H₂O/(Al+P)</i>	30
<i>P/Al</i>	0.8, 0.9
<i>[Si/(Al+P)]</i>	[0.2, 0.1, respectively]

Table 4: Experimental design for the direct hydrothermal synthesis of Cu-SAPO-34 using different amounts of Cu-complex (Cu-TEPA) in combination with a cooperative OSDA (diethylamine, DEA). (T = 150°C static conditions)

Variable	Values
<i>Cu-TEPA/(Al+P)</i>	0.05, 0.1, 0.15, 0.2
<i>[DEA/(Al+P)]</i>	[0.45, 0.4, 0.35, 0.3, respectively]
<i>H₂O/(Al+P)</i>	10
<i>P/Al</i>	0.8, 0.9
<i>[Si/(Al+P)]</i>	[0.2, 0.1, respectively]
<i>Time (days)</i>	1, 7

Table 5: Chemical and elemental analyses of Cu-SAPO-34 samples achieved by using Cu-TEPA and DEA as OSDAs

Sample	Si/(P+Al)	Cu/(P+Al)	%wt Cu	C/N_{real}	% DEA	% TEPA
SAPO-7	0.23	0.04	3.4	2.05	20.8	79.2
SAPO-8	0.24	0.07	6.0	1.77	8.3	91.7
SAPO-9	0.22	0.12	10.4	1.73	4.2	95.8

References:

-
- [1] V.I. Parvulescu, P. Grange, B. Delmon, *Catal. Today* 46 (1998) 233-316.
- [2] R.M. Heck, R.J. Farrauto, S.T. Gulati, "Catalytic Air Pollution Control"; Wiley Intersciences: New York, 2002.
- [3] (a) P. Forzatti, L. Lietti, *Heter. Chem. Rev.* 3 (1996) 33-51; (b) S. Brandenberger, O. Kröcher, A. Tissler, R. Althoff, *Catal. Rev. Sci. Eng.*, 50 (2008) 492-531.
- [4] E. Jacob, R. Müller, A. Schneeder, T. Cartus, R. Dreisbach, H. Mai, M. Paulus, J. Spengler, in *Motortechnische Zeitschrift* (2006) 67.
- [5] (a) R.Q. Long, R.T. Yang, *J. Catal.* 188 (1999) 332-339; (b) R.Q. Long, R.T. Yang, *J. Am. Chem. Soc.* 121 (1999) 5595-5596.
- [6] M. Iwamoto, H. Furukawa, Y. Mine, F. Uemura, S.I. Mikuriya, S. Kagawa, *J. Chem. Soc. Chem. Commun.* (1986) 1272-1273.
- [7] (a) B. Modén, P. Da Costa, B. Fonfé, D.K. Lee, E. Iglesia, *J. Catal.* 209 (2002) 75-86; (b) M.H. Groothaert, J.A. van Bokhoven, A.A. Battiston, B.M. Weckhuysen, R.A. Schoonhetdt, *J. Am. Chem. Soc.* 125 (2003) 7629-7640; (c) I. Melian-Cabrera, S. Espinosa, J.C. Groen, B. Van de Liden, F. Kapteijn, J. A. Moulijn, *J. Catal.* 238 (2006) 250-259; (d) A. Corma, V. Fornés, A.E. Palomares, *Appl. Catal. B*, 11 (1997) 233-242; (e) A. Corma, A. Palomares, F. Marquez, *J. Catal.* 170 (1997) 132-139.
- [8] I. Bull, R.S. Boorse, W.M. Jaglowski, G.S. Koermer, A. Moini, J.A. Patchett, W.M. Xue, P. Burk, J.C. Dettling, M.T. Caudle, U.S. Patent 0,226,545 (2008).
- [9] (a) D.W. Fickel, E. D'addio, J.A. Lauterbach, R. Lobo, *Appl. Catal. B*. 102 (2011) 441-448; (b) I. Bull, R.S. Boorse, W.M. Jaglowski, G.S. Koermer, A. Moini, J.A. Patchett, W.M. Xue, P. Burk, J.C. Dettling, M.T. Caudle, U.S. Patent 0,226,545 (2008); (c) J.H. Kwak, R.G. Tonkyn, D.H. Kim, J. Szanyi, C.H.F. Peden, *J. Catal.* 275 (2010) 187-190; (d) S.T. Korhonen, D.W. Fickel, R.F. Lobo, B.M. Weckhuysen, A.M. Beale, *Chem. Commun.* 47 (2011) 800-802.
- [10] D.W. Fickel, R.F. Lobo, *J. Phys. Chem. C*. 114 (2010) 1633-1640.
- [11] (a) L. Ren, L. Zhu, C. Yang, Y. Chen, Q. Sun, H. Zhang, C. Li, F. Nawaz, F-S. Xiao, *Chem. Commun.* 47 (2011) 9789-9791; (b) L. Ren, Y. Zhang, S. Zeng, L. Zhu, Q. Sun, H. Zhang, C. Yang, X. Meng, X. Yang, F-S. Xiao, *Chin. J. Catal.* 33 (2012) 92-105.
- [12] S.Y. Chung, S.H. Oh, M.H. Kim, I.S. Nam, Y.G. Kim, *Catal. Today*. 54 (1999) 521-529.
- [13] B.M. Lok, C.A. Messina, R.L. Patton, R.T. Gajek, T.R. Cannan, E.M. Flanigen, *J. Am. Chem. Soc.*, 106 (1984) 6092-6093.
- [14] (a) T. Ishihara, M. Kagawa, F. Hadama, Y. Takita, *J. Catal.* 169 (1997) 93-102; (b) H-X. Li, W.E. Cormier, B. Moden, US2008/0241060 (2008); (c) P.J. Andersen, J.E. Collier, J.L. Casci, H-Y. Chen, J.M. Fedeyko, R.K.S. Foo, R.R. Rajaram, WO2008/132452 (2008).
- [15] (a) B.I. Palella, M. Cadoni, A. Frache, H.O. Pastore, R. Pirone, G. Russo, S. Coluccia, L. Marchese, *J. Catal.* 217 (2003) 100-106; (b) A. Frache, M. Cadoni, S. Coluccia, L. Marchese, B. Palella, R. Pirone, P. Ciambelli, *Stud. Surf. Sci. Catal.* 135 (2001) 328; (c) I. Bull, U. Muller, US2010/0310440A1 (2010).
- [16] U. Deka, I. Lezcano-Gonzalez, S.J. Warrender, A. Lorena, P.A. Wright, B.M. Weckhuysen, A.M. Beale, *Microp. Mesop. Mater.* (2012), doi: <http://dx.doi.org/10.1016/j.micromeso.2012.04.056>.

-
- [17] G.Liu, P. Tian, J. Li, D. Zhang, F. Zhou, Z. Liu, *Microp. Mesop. Mater.* 111 (2008) 143-149.
- [18] A.M. Prakash, S. Unnikrishnan, *J. Chem. Soc., Faraday Trans.* 90 (1994) 2291-2296.
- [19] G.Liu, P. Tian, Y. Zhang, J. Li, L. Xu, S. Meng, Z. Liu, *Microp. Mesop. Mater.* 114 (2008) 416-423.